Journal of Thermal Analysis and Calorimetry (2021) 143:1139–1155
https://doi.org/10.1007/s10973-020-09362-y

One-pot sonochemical synthesis route for the synthesis of ZnO@TiO_2/DW hybrid/composite nanofluid for enhancement of heat transfer in a square heat exchanger

Waqar Ahmed[1,2] · S. N. Kazi[2] · Z. Z. Chowdhury[3] · Mohd Rafie Johan[3]

Received: 2 November 2019 / Accepted: 19 January 2020 / Published online: 13 February 2020

Abstract
The thermophysical properties of ZnO@TiO_2/DW composite nanofluids with (0.1, 0.075, 0.05 and 0.025)mass% concentrations have been experimentally studied. The equal and homogenous dispersion of both ZnO and TiO_2 nanoparticles with 50:50 ratio each in distilled water (DW) was attained by the sonochemical method. The efforts are directed to examine the effective thermal conductivity of the different mass% concentrations of ZnO@TiO_2/DW composite nanofluid for a selected range of temperatures at 20 to 45 °C. The maximum improvement in thermal conductivity for ZnO@TiO_2/DW composite nanofluid was noticed for 0.1 mass% concentration, and the maximum enhancement was spotted 47% higher than the base fluid (DW). The heat transfer properties of ZnO@TiO_2/DW composite nanofluids with (0.1, 0.075, 0.05 and 0.025) mass% concentrations and base fluid (DW) in a square heat exchanger were also investigated. Average and local heat transfer values and growth in Nusselt values were conquered for different velocities and corresponding to specific Reynolds numbers range from 4550 to 20,360. The maximum improvement increases about 57% in average heat transfer (h) and Nusselt numbers correspondingly, while local heat transfer for 0.1 mass% is about 500 to 1750 W m^{-2} K, for 0.075 mass% is 500 to 1500 W m^{-2} K, for 0.05 mass% is 500 to 1370 and for 0.025 mass% is 500 to 1150 of the composite nanofluid which is greater than base fluid (DW). The ZnO and TiO_2 mixture gives the best combination to enhance the overall heat transfer coefficient (h).

✉ Waqar Ahmed
waqarum.ah@gmail.com

✉ S. N. Kazi
salimnewaz@um.edu.my

[1] Institute of Advance Studies, University of Malaya, 50603 Kuala Lumpur, Malaysia

[2] Department of Mechanical Engineering, Faculty of Engineering, University of Malaya, 50603 Kuala Lumpur, Malaysia

[3] Nanotechnology and Catalysis Research Center (NANOCAT), University of Malaya, Kuala Lumpur, Malaysia

Graphic abstract

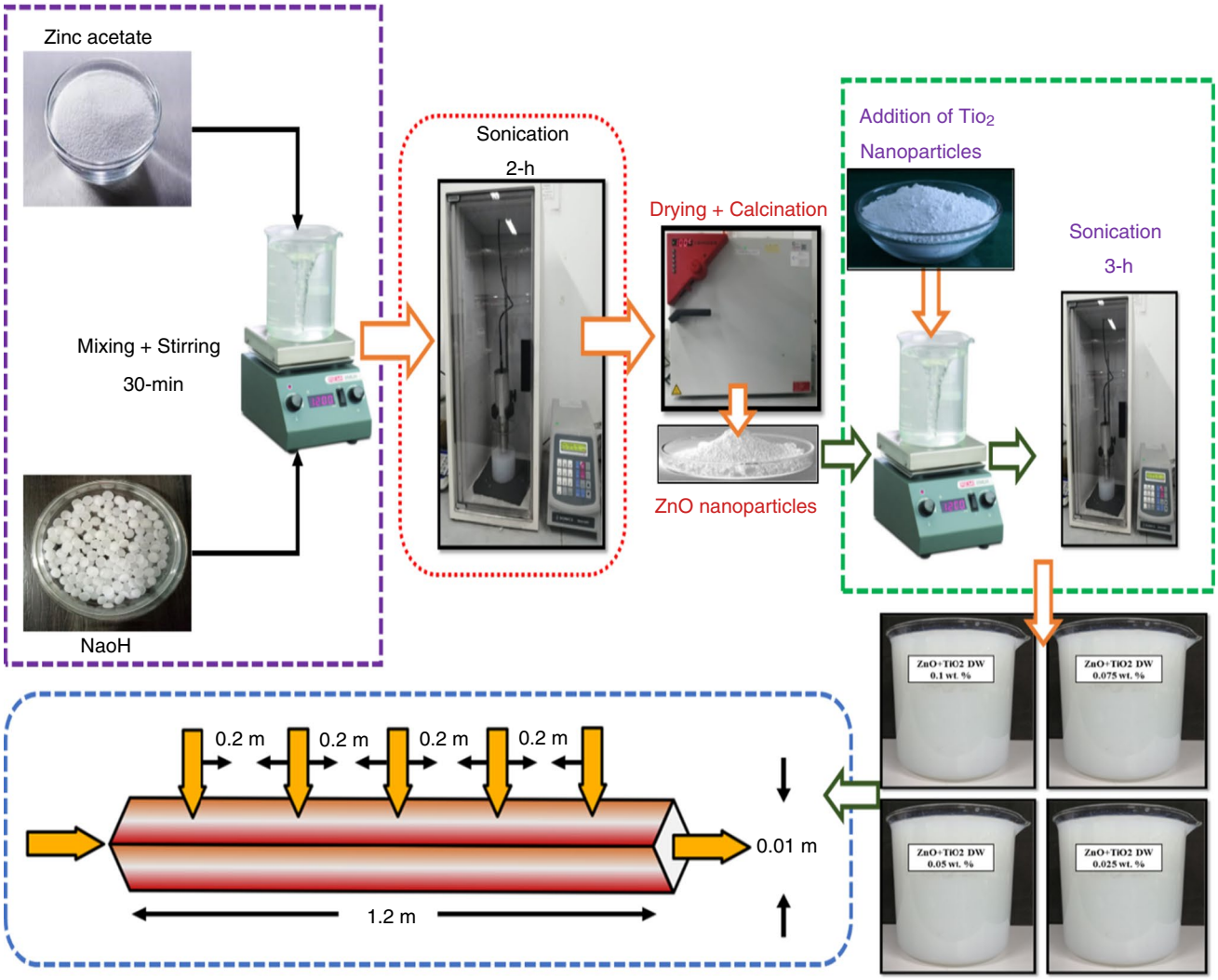

Keywords Nanoparticles · Heat transfer · ZnO@TiO_2 composites · Nanofluids · Thermal conductivity · Heat transfer coefficient

Introduction

It is recognized, the particle size can change the properties of the material and it can be used for numerous applications. In this background, nanomaterials/nanoparticles have a vast scope and tremendous applications in daily life science. One of the fastly growing field of nanotechnology is the cooling and heating in engineering industries. The conventional base fluids are SAE oil, PALM oil, paraffin oil, diathermic oil, PAO oil, vegetable oil, transformer oil, water and ethylene glycol (EG). However, all these conventional base fluids offer low thermal conductivity significantly for an effective cooling system [22]. Due to the expanding worldwide energy challenges, there are many ventures that need proficient heat transfer fluids. As we know, solids have greater thermal conductivity compared to fluids, and various investigations were accomplished to produce small-scale and nanomaterial-dispersed fluids. Because of the issues identified with quick sedimentation, thermal conductivity, clogging and so forth, the endeavor was not completely fruitful. In 1993, Choi and associates have started thinking about another category of fluids utilizing nanoparticles. Parallelly, a Japanese group of scientists introduced metal oxide-based dispersed nanofluid. As the name demonstrates, these are the fluids made by dispersed nanoparticles in the traditional base fluid. As we know, the nanoparticle size is less than microparticles, so

the issues occurred in microfluids can not be happend into nanofluids [8, 49].

Nanoparticles offer higher dispersibility, greater surface area and longer stability in base fluids as compared to microparticles. The nanoparticles provide thousands of time greater volume and surface area ratio than microparticles. The greater surface area of nanoparticles in base fluids improves heat transportation and conduction. There was a variety of hypothetical models for the calculation and improvement in thermal conductivity before nanofluids invention. However, those models deploy only on microparticles and microfluidics. There was a dissimilarity between experimental outcomes and hypothetical models due to the quick sedimentation [33, 18]. The major issue is that microscale or microchannel particles lead to quick sedimentation, which drops down the thermal conductivity and heat transfer efficiency. The optimized use of nanofluids, their synthesis and characterization may approach to the higher efficiency level for all its thermophysical properties [13, 42]. Different researchers presented nanofluids offer not only higher thermal conductivity but also higher heat transfer properties as compared to the base fluids. Nanofluids must contain equal and homogeneous dispersion, higher stability, enhanced thermal conductivity and greater heat transfer ratio [44, 9]. Mainly, the rate of heat transfer is ever dependent upon viscosity, density, dynamic viscosity, thermal conductivity, shape, size of medium and particle morphology as well. Numerous studies on metal oxide-based nanofluids like ZnO, Al_2O_3, TiO_2, SiO_2, MgO, CuO, Fe_2O_3, etc., presented positive enhancement in thermal conductivity and heat transfer efficiency also [31, 48].

To enhance the thermophysical properties of metal oxide, carbon nanoparticles and their composite base nanofluids, a lot of studies with a variety of nanoparticles and efforts were directed by different researchers [38, 1, 19, 35]. Many investigations in the engineering field have proven a positive improvement in heat transfer by using nanofluids for cooling, heat exchanger, solar energy, lubrication, etc. [34]. Nanofluids are the dilute suspension of nanoparticles having a particle size less than 100 nm which are equally distributed in the base fluid [25, 30, 7]. The improvement in nanofluids turns over to the hybrid- or composite-based nanofluids. A lot of experimentations have performed on the thermophysical properties of composite nanofluids for heat transfer augmentation. But still, a research gap could not be filled to meet these challenges [5, 32, 17].

In the earlier time, the scientist was focusing on the betterment of different thermophysical properties of solo nanofluids. Here, the nanocomposites/hybrid-based nanofluids are introduced to achieve higher thermal conductivity and heat transfer properties [21, 23]. Some of the investigations have exposed composites nanoparticles mixed with water as a base fluid can increase the overall heat transfer and thermal conductivity. The rheological properties of TiO_2 and SiO_2 nanoparticles dispersed in distilled water with different ratios are inspected consequently [14]. The efforts were conducted for 1 vol.% concentrations of $TiO_2 + SiO_2$ of the nanoparticles with 80:20, 60:40, 40:60, 50:50 and 20:80 mass% ratios. The 20:80 mass% ratios give the highest value of thermal conductivity with temperature variation 30–80 ℃, and then, finally 16% improvement was achieved greater than base fluid outcomes. With the same efforts, 20:80 ratio gives us the highest heat transfer outcome as compared to others [4, 41]. Hybrid or composite nanofluids are a new idea to enhance the thermal conductivity and heat transportation in engineering field. The composite/hybrid is the mixtures of two or more nanoparticles, where they are mixed or physically blended by different procedures to disperse in base fluid. The mixing or blending process continuously runs, until equal dispersion and the homogeneous stable mixture could not achieve.

The significant intentions of this study are to prosper the real transportation of heat transfer in a square heat exchanger by using ZnO@TiO_2/DW composite nanofluids with different mass% concentrations like (0.1, 0.075, 0.05 and 0.025). The ZnO nanoparticles have been synthesized by using one-pot sonochemical synthesis technique and prepared ZnO- and TiO_2-based composite nanofluids. Further, the experiments were conducted to study the effect of sonochemically synthesized ZnO@TiO_2/DW composite nanofluid on heat transfer growth in a square heat exchanger. The local heat transfer, average heat transfer, local Nusselt numbers, average Nusselt numbers and thermal conductivity in a square heat exchanger at different points are the major focus of this research by using a composite of two different metal oxides. To find the effective enhancement in heat transfer, the Reynolds numbers from 4550 to 20,367 were selected with different velocities and constant heat flux boundary conditions.

Materials and methodology

One-pot sonochemical synthesis route for ZnO

Single-pot sonochemical procedure was used to synthesize the zinc oxide. In this distinctive synthesis procedure, zinc acetate precursor is diluted in a 100-mL mixture of both distilled water and ethylene glycol (EG@DW) with equal mass% of 50:50 conferring to 2:1 molarity under constant magnetic stirring for 30 min. Sodium hydroxide was added in mixture of distilled water and ethylene glycol with (50:50) mass% ratio each under continuous stirring for 30 min. Further, the sodium hydroxide solution was added dropwise into the zinc acetate solution under constant probe sonication. The sonicator power was maximum kept at 750 W, the wave amplitude was adjusted at 80% with 3/2 on and off

time, and the net distributed energy and input power were 36,000 joules and 220 V correspondingly [14, 15]. During the addition of sodium hydroxide solution into zinc, white precipitates initially were seemed in the (DW) base solution. As time passes, it distorted into dense white precipitates. The bulk mixture was then sonicated for 2 h uninterruptedly deprived of using any other coolant. Finally, the reaction was completed and all the white precipitates become dense liquid. The formed white precipitates then washed with distilled water for several times with the help of centrifuge machine at 6000 rpm and lastly washed by ethanol. Then, precipitates were dried in a vacuum oven for 12 h at 60 °C temperature. To get a discrete morphology and a precise shape of the ZnO nanoparticles, the mixture was required to calcine for minimum 3 h sequentially at 200 °C [3, 37, 40]. The Fig. 1 shows a line flow of soncohemical synthesis of ZnO.

Preparation of ZnO@TiO_2/DW composite nanofluids

The presented research is about the composites of ZnO- and TiO_2-based nanofluids for the enhancement of heat transfer in a square heat exchanger. The ZnO was synthesized by a single-pot sonochemical technique, while TiO_2 was procured by chemical provider company Sigma-Aldrich. Further, the ZnO@TiO_2/DW composite nanofluids were prepared for 0.1 mass% concentration by mixing both ZnO and TiO_2 with equal amount in the base fluid (DW). Both ZnO and TiO_2 were physically blended with equal quantity (50:50) each in base fluid (DW) with the mass% concentrations (0.1, 0.075, 0.050 and 0.025) correspondingly. This composite mixture was sonicated for 3 h consecutively to attain well and homogeneous dispersion of nanoparticles in base fluid (DW) [41]. The examinations were directed at four different nanoparticle composite ratios (0.1, 0.075, 0.050 and 0.025) mass%, respectively. Additionally, the offered outcomes show the well-dispersed and -suspended ZnO and TiO_2 in the base fluid (DW). Later, the dilution process is started with the aid of Eqs. (1) and (2), where V1 and V2 are documented to verbalize the nanofluid samples at different mixture ratios and 0.1 mass% concentrations [20, 43]. The detailed preparation procedure is shown in Fig. 2, while Fig. 3 shows the four different (0.1, 0.075, 0.05 and 0.025) mass% concentrations of ZnO@TiO2/DW-based nanofluids as labeled on it.

$$\emptyset = \frac{\omega \rho bf}{\left(1 - \frac{\omega}{100}\right)\rho p + \frac{\omega}{100} * \rho bf} \tag{1}$$

$$\Delta V = (V2 - V1) = V1\left(\frac{\emptyset 1}{\emptyset 2} - 1\right) \tag{2}$$

Test section geometry

Figure 4 shows the schematic view of square heat exchanger made up of stainless steel with 1.2-m total length and 0.01-m diameter. All the surfaces of the given

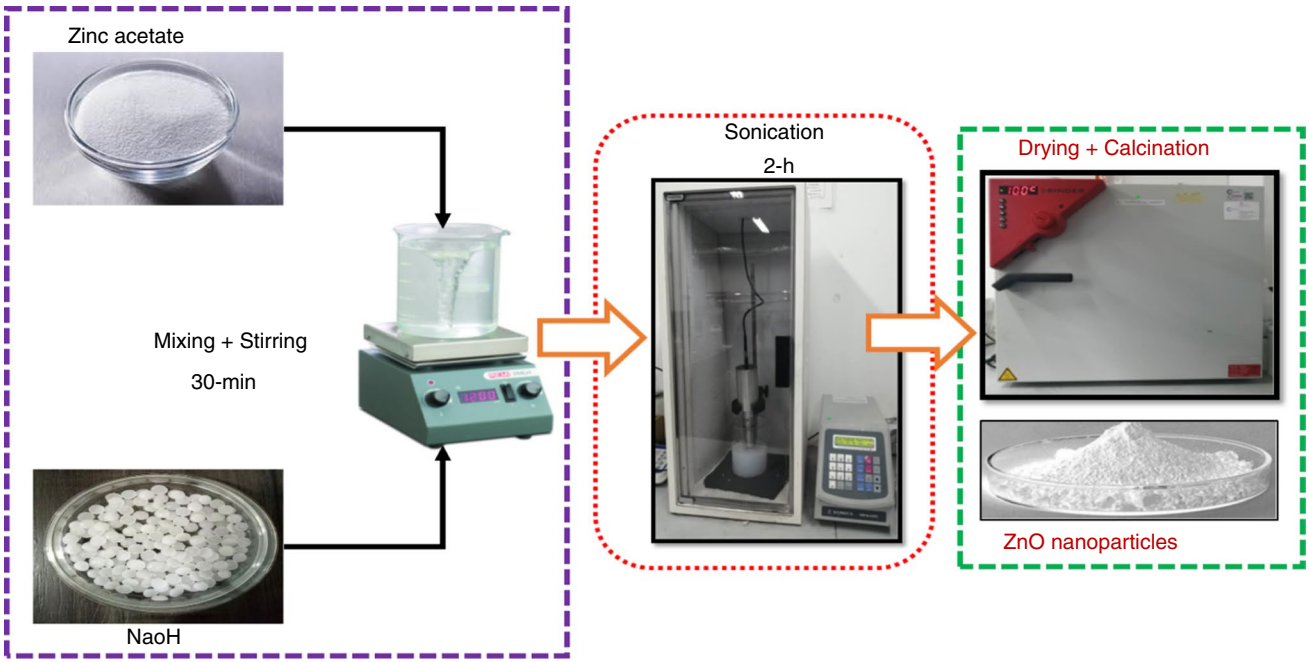

Fig. 1 One-pot sonochemical synthesis of zinc oxide nanoparticles

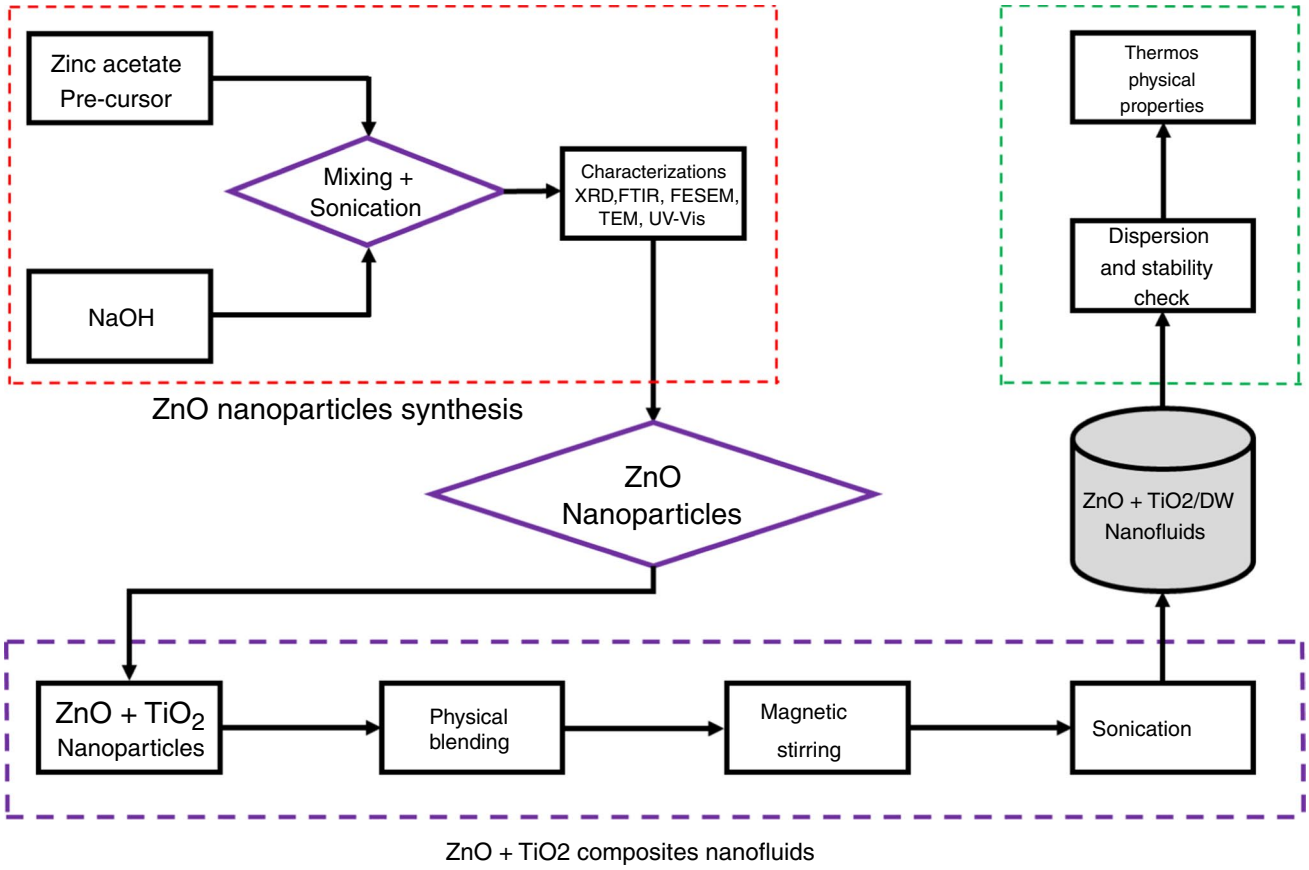

Fig. 2 Preparation of ZnO@TiO_2/DW composite nanofluid by using two-step technique

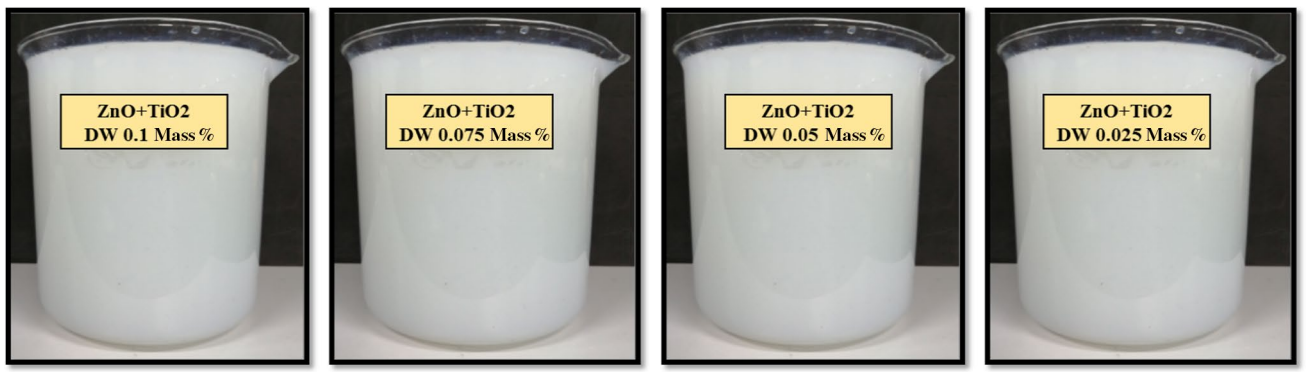

Fig. 3 Different mass concentrations of ZnO@TiO_2/DW composite nanofluids

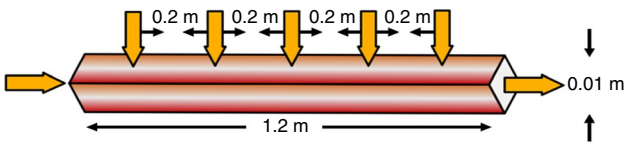

Fig. 4 Geometric view of the square heat exchanger with five K-type thermocouples

heat exchanger are equal and well polished with particular coating materials. Five highly sensitive K-type thermocouples were attached to the heat exchanger surface apart from each other with an equal distance of 0.2 m. Close to the heat exchanger input and output, an inlet and outlet temperature sensors are also attached with this test section to compute the incoming and outgoing temperature values.

Experimental

To see the effects of heat transfer on ZnO@TiO_2/DW composite nanofluid in the square heat exchanger, a well-calibrated and accurate experimental apparatus is needed. In Fig. 5a, a complete test rig with different measuring and calibrating instruments has shown. The experimental setup includes chiller, power panel, control panel, voltage regulator, circuit breakers, control valves, flow meter, fluid control valve, opening and closing valves, circular and square test sections, data logger, pressure meter and sensitive thermocouples on to the surface of the test section. Before starting the experiment, proper calibration and arrangements of each part are necessary to make ensure the proper installation. Further, we attached the thermocouples at various positions with equal distance distribution along the square heat exchanger by following the Wilson model [28, 24]. Moreover, by using this detailed setup we can measure the thermophysical characteristics of ZnO@TiO_2 composites nanofluid by scheming the pressure drop (Pa/m), Nusselt numbers, local and average convective heat transfer (h) and friction factor. By implementing the Newton law for cooling for input and output temperatures and their difference, test section surface temperature and nanofluid temperature, we can calculate the total heat transfer amount.

Characterizations of ZnO@TiO_2/DW binary composite nanofluids

UV–Vis spectra analysis

UV–Vis analysis was conducted to comprehend the optical performance of the sonochemically synthesized ZnO, TiO_2 and binary composites of both ZnO@TiO_2 discretely. The UV–visible outcomes for all samples with mass% of 0.025 concentration are shown in Fig. 6. The prominent peak at 370 nm stipulates the accurate synthesis of Zinc oxide, which is owed to the shifting of blue lateral to the zinc oxide particles in the majority. The maximum absorption level for ZnO was recorded 2.1%. Similar examinations of nanofluids stability and dispersion by UV–Vis analyzer were previously recommended [45, 47]. The absorbance peaks for TiO_2 and binary composites of both ZnO and TiO_2 can also be seen in Fig. 6 correspondingly. The highest peak between 300 and 400 nm and the 1.5 absorbance % show the nature of TiO_2 nanoparticles. Same as this, the obtained peak behind 300 nm and absorbance % about 3.5 show the nature of both Zno@TiO_2 composites. The outcomes confirm the good dispersion and suspension of all nanoparticles in the base fluid (DW). The composite nanofluids give the highest absorbance level as compared to other particles due to their extended

Fig. 5 Experimental setup with different parts for heat transfer measurements

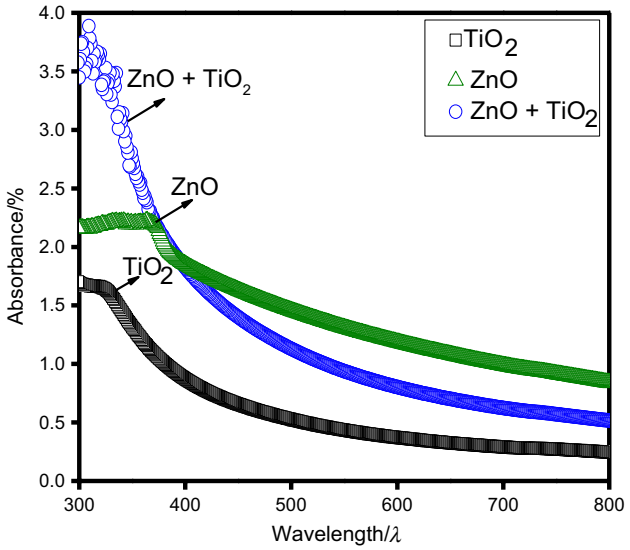

Fig. 6 UV–Vis analysis profile for ZnO, TiO_2 and ZnO@TiO_2 binary composite nanofluids

interfacial zone among all particles. The longer stability and suspension of nanoparticles in a base fluid depend upon the use of any surfactant or sonication time as well [39, 51].

FESEM analysis of ZnO@TiO/DW composite nanofluids

The FESEM analysis was conducted to perceive the morphology of particles and their equal dispersion in the base fluid (DW). The equal ratio of both nanoparticles ZnO and TiO_2 (50:50) of each was dissolved in a base fluid and sonicated for 2 h. The FESEM images for ZnO and TiO_2 composite nanofluids at 0.1 mass% concentration are given in Fig. 7. From the FESEM images, the morphology and dispersion of ZnO, TiO_2 and their composite can be observed, respectively. Figure 7a shows the ZnO nanoparticles by using 10.00 kV HV, max magnification 50,000 setup, (b) shows the TiO_2 nanoparticles cloud, and (c) shows the composites of both nanoparticles with equal dispersion in the base fluid. The average particle size of ZnO nanoparticles is 17 nm and TiO_2 is 21 nm, respectively. Generally, the proper coordination of both nanoparticles highly depends on the mass% ratios of the composites, which describes the % of each nanoparticle in the base fluid (DW). The smaller nanoparticles help to fill the space among large size nanoparticles, and this may enhance the thermophysical properties, specific heat and thermal conductivity of composite nanofluid. Further, due to this condition viscosity and density can also be changed. However, to find the specific characteristics of both nanoparticle dispersion and stability, the current research offers the mixture ratio of nanoparticles' thermal conductivity and heat transfer through a square heat exchanger [16, 46].

Result and discussions

Thermal conductivity of ZnO@TiO_2/DW composite nanofluids

Figure 10 shows the relations among thermal conductivity of ZnO@TiO_2 composites with different values of temperature for (0.1, 0.075, 0.05 and 0.025) mass% concentrations. The thermal conductivity outcomes of ZnO@TiO_2/DW composite nanofluids for each mass% ratio have increased with the increase in temperature degree and deliberately more than associated with base fluid. Also, it has been observed that the highest thermal conductivity was recorded with a mass ratio of 50:50 of both zinc oxide and titanium oxide for 0.1 mass% concentration. In the meantime, the 0.025 mass% carried the lowest thermal conductivity among all other composites mass% concentrations. The outcomes inveterate that the increase in mass% of both metal oxide nanoparticles pays an equal contribution to the higher thermal conductivity of ZnO@TiO_2/DW composite nanofluids as shown in Fig. 8a. In the present efforts, the relation between nanoparticle composites mass% to the thermal conductivity development may be due to the different sizes of each nanoparticle and the mass quantity of the smaller nanoparticles present in the composite. The confirm particle size of ZnO is 17 nm, which is less than the TiO_2 particles of 21 nm. The ZnO particles help to enhance the thermal conductivity by filling the space among the large size TiO_2 nanoparticles, as shown in FESEM images in Fig. 7. The mixing process of both nanoparticles in the composite liquid will increase the interactions area for thermal conduction among the unlike molecules and hence influence the higher thermal heat transfer which occurs during the colloidal suspension due to Brownian motion [26, 36, 27].

The rise in effective thermal conductivity of ZnO@TiO_2/DW composite nanofluids with different mass% ratios associated with a series of temperatures can be seen in Fig. 8b disparately. The results reveal that the effective thermal conductivity is increasing with an increase in the mass% of ZnO and TiO_2 nanoparticles in the mixture of ZnO@TiO_2/DW composite nanofluids, except 0.025 mass% ratio which shows the lowest value of the thermal conductivity. The effect of temperature variations on thermal conductivity can be seen in the below graph. Furthermore, the maximum 47% enhancement is achieved with the highest value of temperature 45 °C for 0.1 mass% of the composite nanofluid. This improvement is led by the kinetic energy between both nanoparticles and their Brownian motion effects in the base

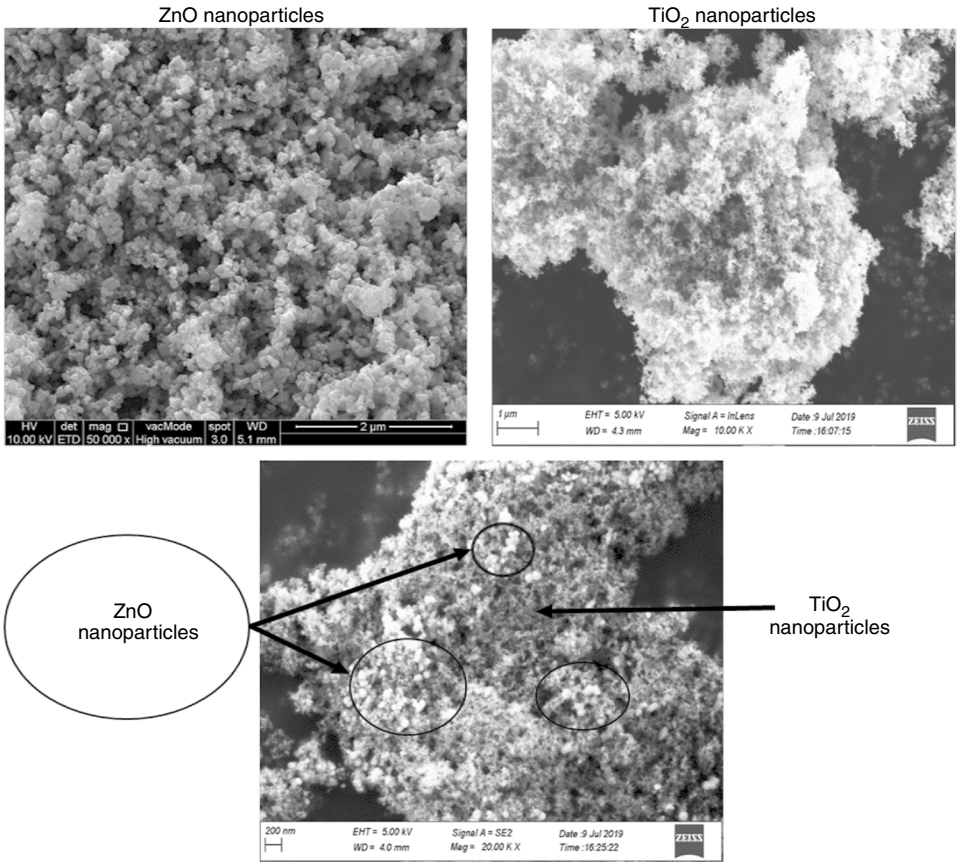

Fig. 7 FESEM images showing equal dispersion of ZnO and TiO_2 and their composites

fluid [50, 2]. Effective thermal conductivity can be expressed mathematically by the following equation.

$$keff = \frac{knf}{kbf} \tag{3}$$

Stability of ZnO@TiO_2/DW composite nanofluids

The ZnO@TiO_2/DW composite nanofluid solution was imperiled to a continuous probe sonication process for 2 h to increase the dispersion and stability of nanoparticles and to minimize the agglomeration. Four samples of 50 mL were prepared according to (0.1, 0.075, 0.05 and 0.025) mass% concentrations and sonicated for 2 h each to get good stability and dispersion [11]. As per Yu et al. [10], the nanofluids seem to be more stable when the nanoparticle size remains small and constant. The physical observations for sedimentation of the ZnO@TiO_2/DW-based composite nanofluids can be seen in Fig. 9. After preparation of the samples, during the week 1 and week 2 all the nanofluids are well dispersed and stable. The maximum stability was noticed for 0.1 mass% owing to the greater amount of nanoparticles. In the week 3, it starts to sediment and slightly goes to settled down. Figure 10 shows the maximum stability time for each concentration without using any surfactant. The complete observations were carried upto 14 days maximum from its preparation time and few images have been shooted during experiment.

Figure 10 shows the stability and dispersion of ZnO@TiO_2/DW composite nanofluids. Four different mass% concentrations of ZnO@TiO_2/DW composite nanofluids like (0.025, 0.05, 0.075 and 0.1) are observed for a couple of weeks. The Fig. 10 shows from week 1 to week 2 all the samples looks well stable and dispersed, and after week 2 it starts to sediment. The sedimentation rate for each sample depends upon the mass% loading of both ZnO and TiO_2 nanoparticles in base fluid (DW) and their sonication time. As the sonication time increased, the dispersion and stability of nanoparticles increased up to a certain level. The declining trend showing the 0.1 mass% still has less sedimentation as compared to other samples, because it has a greater amount of nanoparticles.

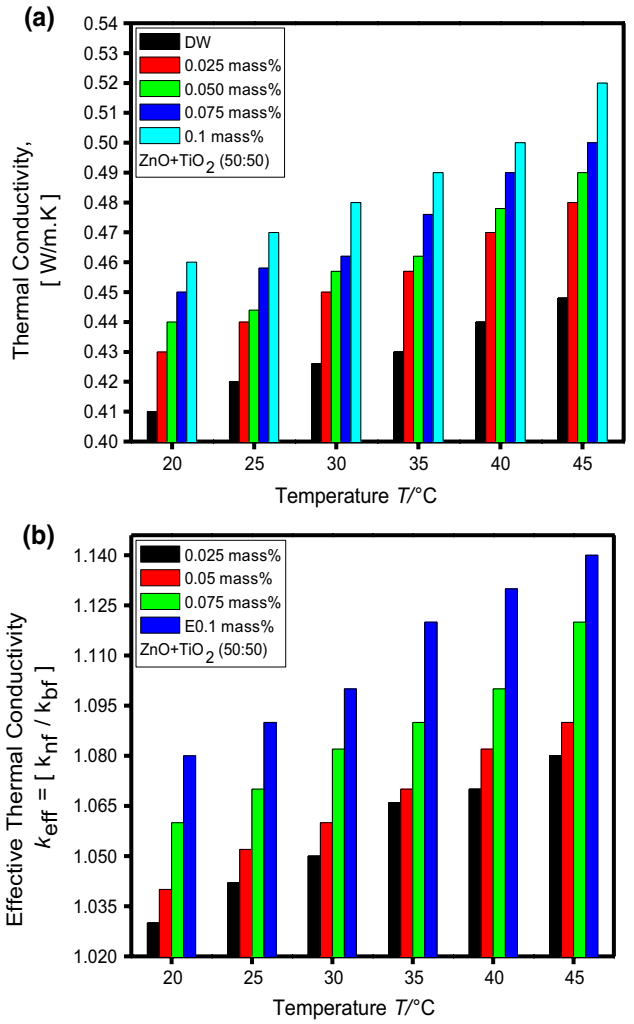

Fig. 8 **a** Improvement in thermal conductivity and **b** maximum enhancement in effective thermal conductivity with an increase in mass% concentrations

Thermophysical and hydrodynamics properties of ZnO@TiO$_2$/DW composite nanofluids

To evaluate the pumping power and pressure drop variations in the square pipe heat exchanger, intentions are accomplished to find out the friction loss for both distilled water and ZnO@TiO$_2$/DW composite nanofluids by using mathematical Eq. (4). The assessed outcomes were coordinated with two different models Petukhov [29] and Blasius's [6] with empirical co-relation, respectively. The tentative friction factor (ff) and output results were promising, since the variances were almost $\leq 5\%$ as associated with the statistics from both Blasius and Petukhov empirical correlations, which shows the square heat exchanger is steady to quantify the change in total pressure drop at different values of the Reynolds numbers specified in this investigation.

$$f = \frac{\nabla P}{\left(\frac{L}{D}\right)\left(\frac{\rho v^2}{2}\right)} \tag{4}$$

The variations in pressure drop alongside the square heat exchanger for ZnO@TiO$_2$/DW composite nanofluids with different mass% concentrations against the constant Reynolds numbers are given in Fig. 11a. The mounting trend of the graph designates as the Reynolds Numbers values increased and the pressure drop will increase as well. The graph shows the pressure drop for each concentration and distilled water also, and in case of base fluid the pressure drop is less across the test section due to nonavailability of the nanoparticles loading. Addition of nanoparticles in the base fluid may cause too little friction, and due to this friction pressure drop will increase alongside the square pipe. Each of ZnO@TiO$_2$/DW composite nanofluid concentration like (0.1, 0.075, 0.05 and 0.025) was treated separately, and the highest pressure drop value noticed for 0.1 mass% is 2400 Mpa. This highest pressure drop amount is subjected due to the greater amount of both ZnO and TiO$_2$ nanoparticles inside the base fluid.

During experimentation, when nanofluid is running inside the square heat exchanger the internal friction will definitely affect to pressure drop, and it may cause to increase or decrease the pressure drop. Basically, this friction effect occurs due to the presence of nanoparticles in the base fluid (DW). The pertinent friction factor (ff) results attained by using mathematical Eq. (10) are also offered against a specific range of Reynolds) numbers in Fig. 11b. The friction factor for base fluid and each of the mass% concentration of ZnO@TiO$_2$/DW composite nanofluid is the main concern of this test. In case of distilled water, a base fluid shows maximum friction factor in square heat exchanger up to 0.037, while it can be noticed in below graph that the friction factor (ff) has augmented about 0.046 for ZnO@TiO$_2$/DW composite nanofluids for 0.1 mass% in concentration. This behavior speculated that it happens due to the presence of the mass% concentrations of both ZnO and TiO$_2$ nanoparticles in the base fluid (DW). The declining trend for friction factor shows once the Reynolds numbers vary from low to higher than friction factor, it will be drop down linearly. Due to the loading of ZnO@TiO$_2$ nanoparticles in the base fluid (DW), its overall viscosity will be increased, which ended the obligation of a minor increase in velocity of nanofluid to maintain the Reynolds numbers constant. At this point, the velocity of ZnO@TiO$_2$/DW composite nanofluids displays a dynamic role to raise the pressure drop value and friction factor in a square heat exchanger. Finally, the highest friction factor and pressure drop were noticed for 0.1 mass% of the ZnO@TiO$_2$/DW composite nanofluids, which happened due to the maximum amount of the nanoparticle

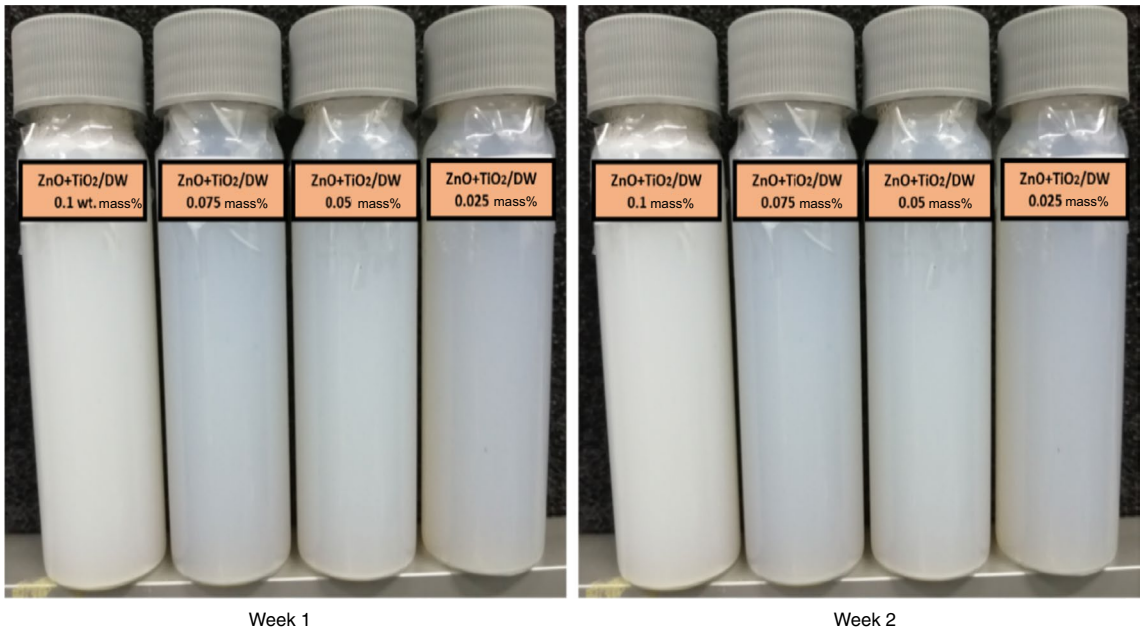

Fig. 9 Stability and dispersion of ZnO@TiO_2/DW composite nanofluids with different mass%

in the base fluid. Figure 11c shows the required pumping power for each of the mass% concentration of the ZnO@TiO_2/DW composite nanofluid during experiment running. The growing trend describes that as the amount of the nanoparticles in the base fluid will increase, the setup needed more power to run the fluid. The maximum pumping power was noticed 1.41 for 0.1 mass% in concentration. As compared to the base fluid, the nanofluid having particle inside shows the need for a greater amount of pumping power. Mathematically, pumping power can be calculated by using the following equation.

$$\frac{Wnf}{Wbf} = \left(\frac{\rho bf}{\rho nf}\right)^2 \left(\frac{\mu nf}{\mu bf}\right)^3 \tag{5}$$

Dynamic viscosity of nanofluids is most important as same as thermal conductivity. Plenty of studies have performed on the thermal conductivity of nanofluids as compared to the dynamic and kinematic viscosities of nanofluids. Different viscosity formulas and models deliberated the mass% concentrations of present nanoparticles in the base fluid to show the effects of viscosity on nanofluids. Figure 11c–d displays the dynamic and kinematic viscosity outcomes of ZnO@TiO_2/DW composite nanofluids with different mass%. The overall dynamic viscosity will decrease with the increase in temperature values. Similarly, the kinematic viscosity will also decrease with the increase in temperature, and the trend is nonlinear due to different particles.

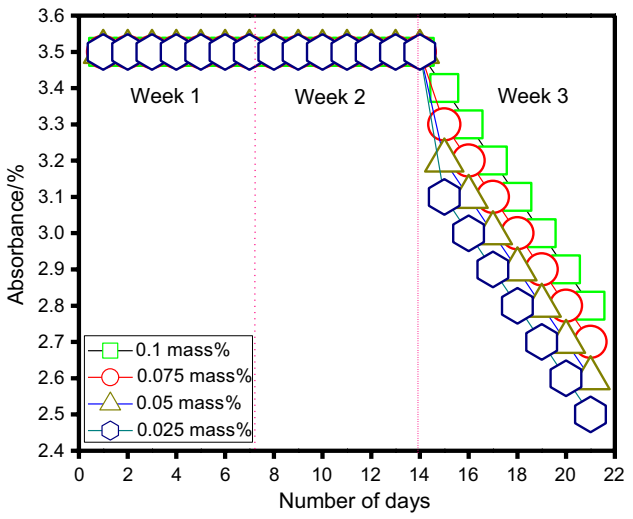

Fig. 10 Absorbance and stability profile for different concentrations of ZnO@TiO_2/DW composite nanofluids for 3 weeks continuously

Improvement in average heat transfer and average Nusselt numbers of ZnO@TiO_2/DW composite nanofluids with different mass% concentrations and distilled water

The previous literature which exposes the growth of different kinds of nanoparticles in any type of base fluids shows enhanced convective heat transfer properties. The stated investigations of the effects of ZnO@TiO_2/DW

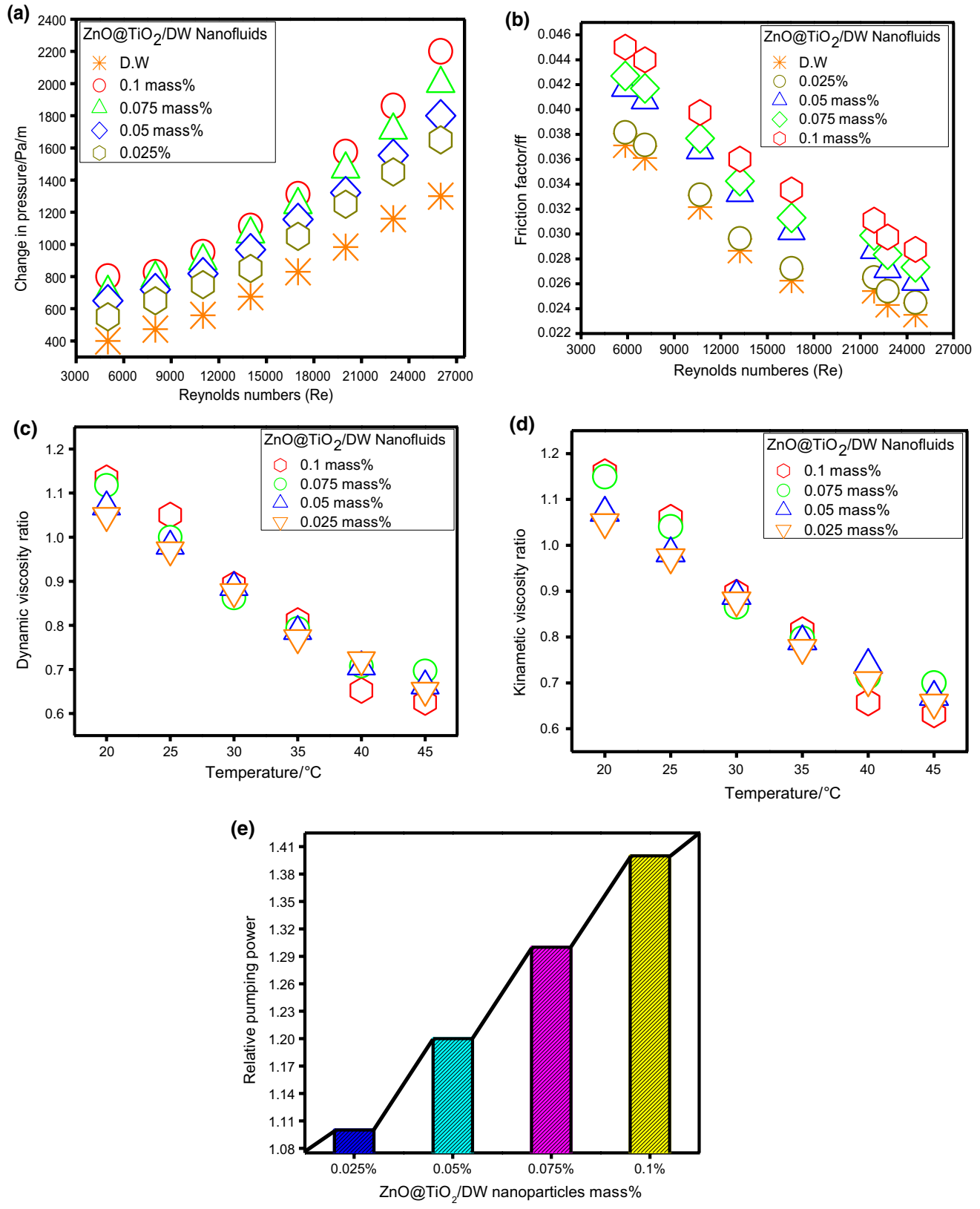

Fig. 11 Hydrodynamic properties, **a** pressure drop against Reynolds numbers, **b** friction loss for each mass% concentration, **c** dynamic viscosity of composite nanofluids, **d** kinematic viscosity of composite nanofluids and **e** pumping power for different concentrations of ZnO@TiO$_2$/DW fluid

composite nanofluids with different mass% (0.1, 0.075, 0.05 and 0.025) concentrations on the local and average heat transfer coefficients values and effective thermal conductivity for given Reynolds numbers from 4550 to 20,360 were conducted. The experimentation was led to evaluate the heat transfer coefficient and thermophysical properties of our ZnO@TiO_2/DW composite nanofluids flowing in a closed square heat exchanger. Calibration of experimental setup is necessary prior to see the inner surface temperature of the test section in order to calculate the maximum presence of heat conduction in the square tube wall as well as convection of the composite nanofluid flowing through the square heat exchanger. Here, we follow the Wilson plot procedure [12], by equating the overall resistance among different points along the direction of heat transfer and inner surface temperature of the square heat exchanger by using some mathematical calculations. We considered the different thermophysical properties of the composite nanofluids and distilled water by using following factors: heat transfer coefficient (h), Nusselt numbers, pumping power and pressure drop. To govern the heat transfer coefficient (h), the Newton law of cooling based on a bulk amount of inlet and outlet temperature and surface is temperature measured from the experimentation. Furthermore, the average heat transfer coefficient was projected for ZnO@TiO_2/DW composite nanofluids in a square heat exchanger separately of the specified mass% for the conclusion with the base fluid (DW). In Fig. 10a, the rising trends are obviously depicting the convective heat transfer (h) which is increasing as the ZnO@TiO_2/DW composite-based nanofluids mass% is increasing. For the base fluid (DW), it can be understood that the heat transfer (h) was less due to the absence of both ZnO@TiO_2 nanoparticles in the water, by means of when nanoparticles were mixed it augmented the average heat transfer coefficient. From Fig. 12a, it can be easily seen at 0.1 mass% concentration, the heat transfer coefficient was higher as compared to distilled water data. In the case of the base fluid (DW), the maximum successive heat transfer was from 600 to 850 (W m^{-2} K), and on the other side with same 0.1 mass% of ZnO@TiO_2/DW composite-based nanofluids the heat transfer coefficient was mounted greater and the outcome varied from 600 to 1250 (W m^{-2} K).

$$Re = \left(\frac{\rho v D}{\mu}\right) \tag{6}$$

Experimentation data have been used to calculate the heat transfer coefficient (h) and the total pressure drop values for ZnO@TiO_2/DW composite nanofluids. Reynolds numbers of distilled water and ZnO@TiO_2/DW composite nanofluids with different variations in mass% concentrations like (0.1, 0.075, 0.05 and 0.025) can be restrained based on the complete experimental setup for heat transfer, mass, velocity and hydraulic diameter of the square heat exchanger by using following mathematical equations.

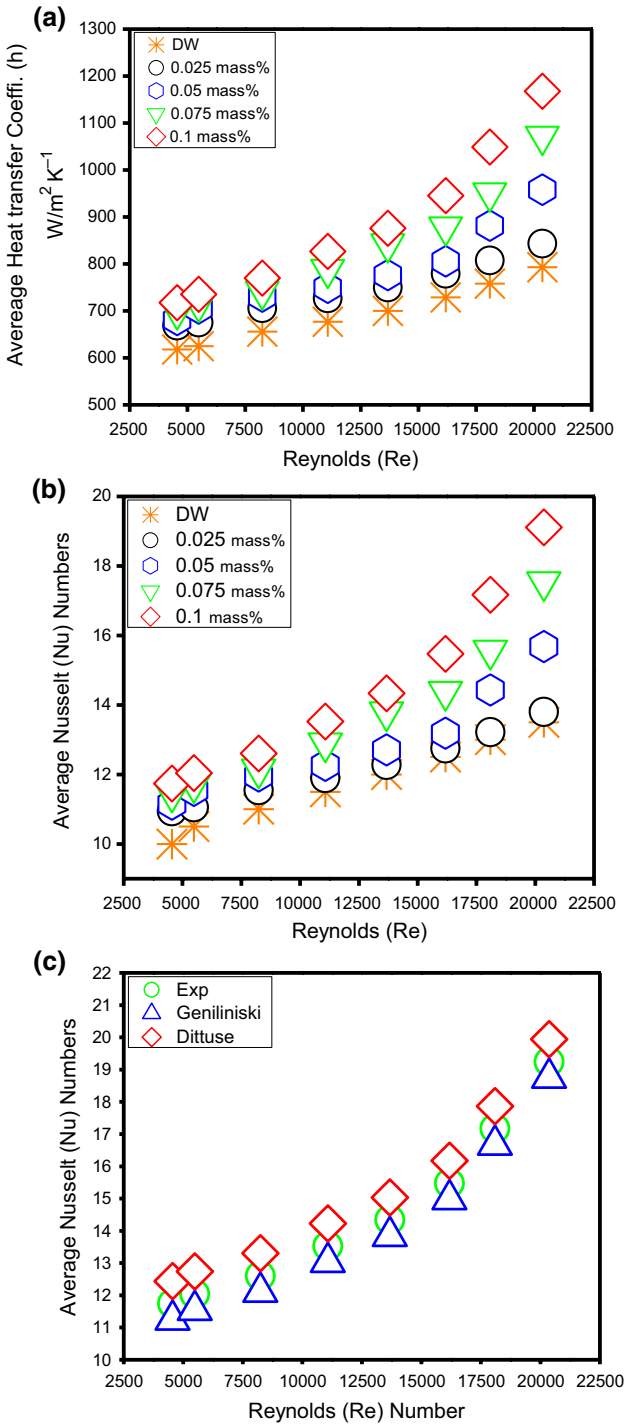

Fig. 12 **a** Growth in average heat transfer and **b** average Nusselt numbers for ZnO@TiO_2/DW composite nanofluids and base fluid (DW) and **c** correlation of experimental data with model data

$$h = \left(\frac{q''}{Tw - Tb}\right) \tag{7}$$

$$q'' = \left(\frac{Q}{A}\right) \tag{8}$$

$$A = L * L \tag{9}$$

On the basis of successive measurement of heat transfer coefficient (h), it is easy to optimize the growth in Nusselt numbers for each concentration of the detailed composite fluid. Figure 12b describes the development in average Nusselt numbers of each mass% concentration of ZnO@TiO_2/DW composite nanofluids according to the variations in Reynolds numbers from 4550 to 20,367 separately. It can be observed that the average Nusselt numbers for the base fluid (DW) varied from 9 to 14 with the rise in Reynolds (Re) values. After mixing both ZnO and TiO_2 nanoparticles in the base fluid (DW), the optimistic enhancement in the Nusselt numbers was professed, which is definitely accredited to the rise in nanoparticles mass% concentrations. With 0.1 mass% ZnO@TiO_2/DW composite-based nanofluid concentration, the highest growth in Nusselt numbers was noticed differing to the Reynolds numbers varying from 4550 to 20,367. The obtained Nusselt numbers were higher as compared to that noted for distilled water due to the addition of nanoparticles in the base fluid. The succeeded Nusselt values were estimated by using the following mathematical relation.

$$Nu = \left(h * \frac{D}{K}\right) \tag{10}$$

$$\mathrm{Nu} = \left(\frac{\left(\frac{f}{8}\right)(\mathrm{Re} - 1000)\,\mathrm{Pr}}{1 + 12.7\left(\frac{f}{8}\right)^{0.5}\left(\mathrm{Pr}^{2/3} - 1\right)}\right) \tag{11}$$

$$Nu = \left(\frac{\left(\frac{f}{8}\right)\mathrm{Re}\,\mathrm{Pr}}{1.07 + 12.7\left(\frac{f}{8}\right)^{0.5}\left(\mathrm{Pr}^{2/3} - 1\right)}\right) \tag{12}$$

Finally, the experimental results were compared with Gnielinski and Dittus models data, which show promising comparison among experimental data and model data. The combination of ZnO@TiO2/DW composite/hybrid nanofluids shows promising heat transfer improvement as compared to model data. Figure 12c shows all the experimental and models data showing growing trend with the increase in Reynolds numbers. Here, these composite/hybrid nanofluids are considered to be the suitable choice for heat transfer applications.

Growth in local heat transfer for different mass% concentrations of ZnO@TiO_2/DW composite nanofluids

The experimentation was led to measure the effects of ZnO@TiO_2/DW composite nanofluid on heat transfer coefficient in the square heat exchanger. The constant heat flux boundary condition and variable flow rate basis strategy have been adopted during the experiment. The effect of composite nanofluids with four different mass% concentrations was recorded locally on different points of square heat exchanger. Figure 13 signifies the local behavior of the heat transfer coefficient for each ZnO@TiO_2/DW composite nanofluids mass% concentration at different points of the square heat exchanger. Each concentration was individually treated by square heat exchangers with different flow rates, and variations in Reynolds numbers were also subjected. During the experimentation, the outcome arises 0.025 mass% concentration of ZnO@TiO_2/DW composite-based nanofluids, and the local heat transfer coefficient (h) was noticed from 600 to 1100 W m^{-2} K at the Reynolds numbers from 4550 to 20,367. In the case of 0.075 mass%, ZnO@TiO_2/DW composite-based nanofluids concentration, the local heat transfer coefficient (h) was perceived from 600 to 1300 W m^{-2} K at the specific range of Reynolds numbers. For 0.05 of ZnO@TiO_2/DW composites based nanofluids mass% concentrations, the heat transfer coefficients (h) were documented from 600 to 1500 W m^{-2} K at the same values of Reynolds numbers. The maximum enhancement in heat transfer coefficient (h) was recorded 600–1750 W m^{-2} K when the mass% concentration of ZnO@TiO_2/DW composite-based nanofluids arises up to 0.1% with the same Reynolds numbers. The conclusion from the current experiment portrays that the presence of both nanoparticles in base fluid (DW) and their mass% increment up to 0.1 mass% imperiled to linear growth in heat transfer in the square heat exchanger.

Growth in local Nusselt numbers for different mass% concentrations of ZnO@TiO_2/DW composite nanofluids

On the basis of the heat transfer coefficient, it is easy to elaborate the changes in Nusselt numbers along the square heat exchanger on different points. Nusselt numbers were estimated for all mass% concentrations by using numeric calculations with the heat transfer coefficient results. Figure 14 articulates the different growing trends in local Nusselt numbers with a specific range of Reynolds numbers from 4550 to 20,367 and different mass% of ZnO@TiO_2/DW composite-based nanofluids like (0.1, 0.075, 0.05 and 0.025) concentrations. Throughout the experiment, it professed that the local Nusselt numbers improved with the increase in Reynolds numbers in a square heat exchanger

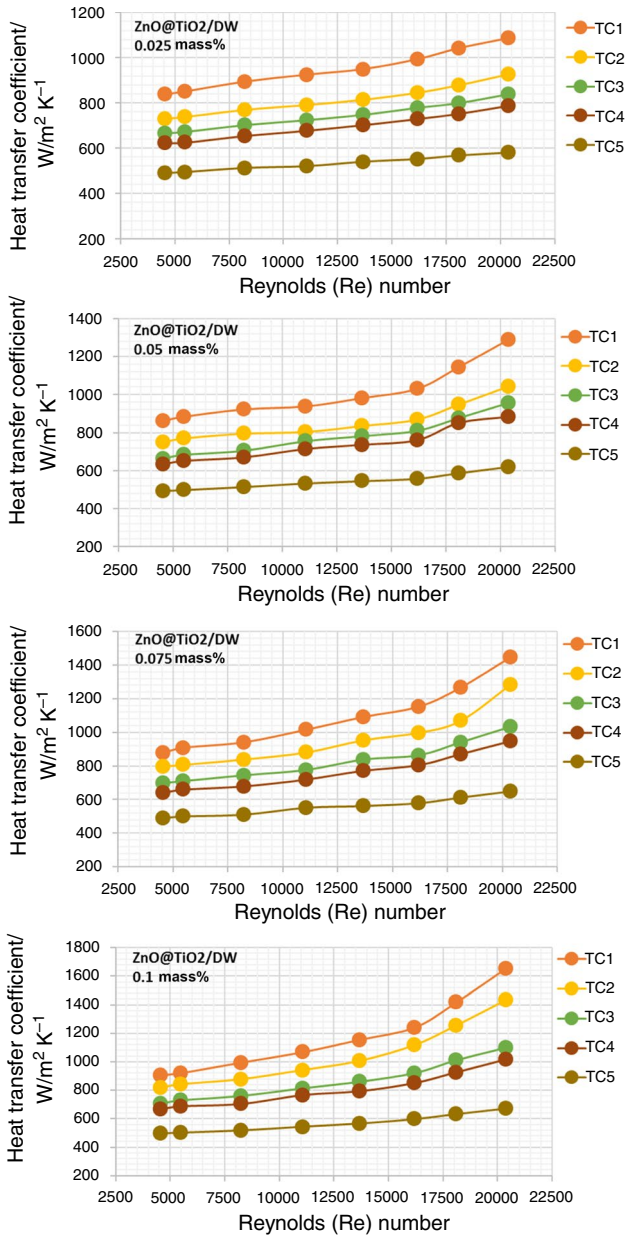

Fig. 13 Effects of ZnO@TiO_2/DW composite of (0.025, 0.05, 0.075 and 0.1) mass% concentrations on local heat transfer improvement at each thermocouple (TC)

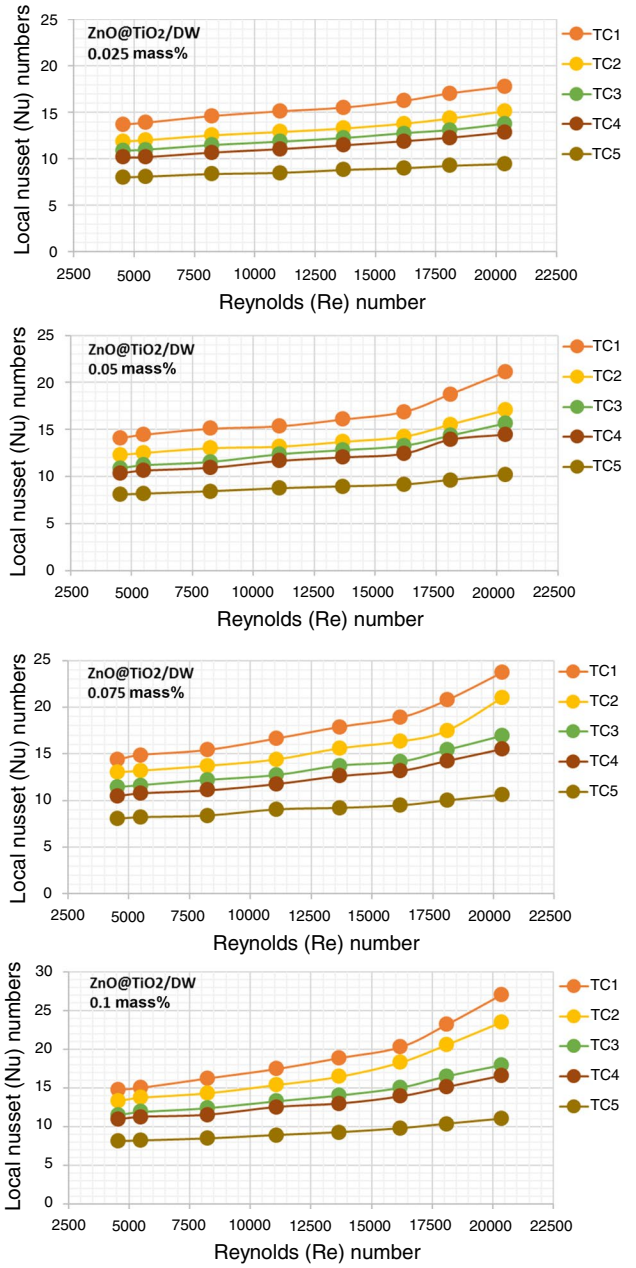

Fig. 14 Effects of ZnO@TiO_2/DW composite with (0.025, 0.05, 0.075 and 0.1) mass% concentrations on local Nusselt numbers growth at each thermocouple (TC)

with the same hydraulic diameter. Also, this growing effect is subjected to change in mass% of both nanoparticles in the base fluid. It can be perceived in Fig. 12 that in all of the presented mass% concentrations of ZnO@TiO_2/DW composite-based nanofluids, the local Nusselt numbers are linearly growing with the change in mass% and variations in Reynolds numbers. For the 0.025 mass% ZnO@TiO_2/DW composite-based nanofluid, the local Nusselt numbers were noticed from 8 to 16 corresponding to the heat transfer coefficient at a given range of Reynolds numbers prolonged from 4550 to 20,367. In the case of 0.05 mass% ZnO@TiO_2/DW composite nanofluid, a growing trend in local Nusselt numbers was noticed from 8 to 21 for the same Reynolds numbers. For the 0.075 mass% of ZnO@

TiO_2/DW composite nanofluid, the observed local Nusselt numbers were spotted from 8 to 24 along with the Reynolds series. Last of all, for the 0.1 mass% of ZnO@TiO_2/DW composite nanofluid mass concentrations a surprising improved trend was seen in the Nusselt numbers ranging from 8 to 28 with specified Reynolds numbers discussed previously. This deteriorating behavior for lower concentrations and Reynolds numbers is accredited to the agglomeration of both ZnO and TiO_2 particles for less value of Reynolds numbers and lower metal oxide surface area for mass% concentrations. With the greater value of Reynolds numbers, the agglomeration for both ZnO and TiO_2 drops down which supports the good dispersion and stability of each nanoparticle in the base fluid (DW) due to its appropriate mixing. Finally, the conclusion comes up with projecting enhancement in Nusselt numbers due to the particles loadings into the base fluid (DW). The outcomes show a maximum improvement with 0.1 mass% of the nanoparticles composite nanofluids.

Uncertainties in experimental setup

Proper arrangement and calibration of experimental setup before running it are the basic need of an experiment. Electrical or electronic equipment may cause to lead the little errors during experiments due to their accuracy limits. To figure out, the total magnitude of this error is necessary during the experiment. The contemporary examinations of ZnO@TiO_2/DW composite nanofluids with different mass% concentrations for heat transfer coefficient measurement, the net velocity, changes in temperature, volume flow, pressure drop, Reynolds numbers, Nusselt numbers, heat transfer coefficient, supplied voltage, current, heat flux, pumping power, ambient temperature, differential pressure, thermal conductivity and effective thermal conductivity were examined with appropriate measuring equipments. All over the experimental measurements of the detailed parameters, the uncertainties/fluctuations happened are offered in Table 1 Seeing the associated errors in each aspect signified by (x_n) error calculations of dependent constraints was taken out by using mathematical Eq. (13). During all experimentations, different inconsistencies were noticed repeatedly which are given in the table with outcome values. Frequent time reiteration approach to express each constraint of proposed experimentations significances, all the values were within the limits of uncertainties.

$$W = \frac{[(x1)2 + (x2)2 + \ldots + (xn)2]}{2} \tag{13}$$

Table 1 Uncertainties tallied during the experiment of the ZnO@TiO_2/DW nanofluids

Parameters	Symbols	Uncertainty/%
Ambient temperature	Te	± 0.16
NF mass flow rate	v	± 1.92
NF differential pressure	h_h	± 2.22
NF thermal conductivity	k_{nf}	± 3.41
NF specific heat measurement	Cp_{nf}	± 3.92
Voltage	V	± 1.15
Current	I	± 1.15
Heat flux	Q	± 1.15
Reynolds numbers	Re	± 3.33
Convective heat transfer	h	± 3.22
Nusselt numbers	Nu	± 3.41
Pumping power	P_P	± 2.44

Conclusions

The effects of thermal diffusivity and momentum of composite nanofluids over thermal conductivity on heat transfer growth in square heat exchanger were investigated here numerically and experimentally. Prior to run the nanofluids, the experimentation has been directed for the base fluid (DW) to validate the numerical model of fluid flow in a square heat exchanger. To validate the experimental setup, the average Nusselt numbers of experimental data were compared with Gnielinski and Dittus models which showed the good connection with experimental data. In the stated investigation, single-pot sonochemical-assisted technique was adopted to synthesize the ZnO nanoparticles, and then, TiO_2 nanoparticles were mixed all together in the base fluid (DW) with 50:50 ratio each to synthesize the ZnO@TiO_2/DW composite nanofluids.

- The four different mass% concentrations of ZnO@TiO_2/DW composite nanofluids like (0.1, 0.075, 0.05 and 0.025) were inspected for heat transfer and other thermophysical properties and their growth in a square heat exchanger.
- Effective thermal conductivity analysis for all mass% concentration of ZnO@TiO_2/DW composite nanofluid was conducted by using advanced KD-2 Pro thermal analyzer. The experiment exposes that the equal quantity of each ZnO and TiO_2 particle in the base fluid (DW) signifies the positive enhancement in the effective thermal conductivity, where the equal amount of ZnO and TiO_2 particles gives the controlled parameters and improves the heat convection in square heat exchanger. The thermal analyzer shows that the maximum enhancement in thermal conductivity was 0.40–0.54 W m^{-2} K and the

47% enhancement was noticed in effective thermal conductivity.

- Further investigations on heat transfer properties of composite nanofluids with a specific range of Reynolds numbers from 4550 to 20,367 were conducted for all mass% concentrations. 0.1 mass% of ZnO@TiO_2/DW composite nanofluids gives the higher thermal performance of the composite nanofluids as compared to other concentrations and the base fluid (DW). Subsequently, average and local heat transfer outcomes for these all mass% concentrations and the base fluid (DW) were assessed with different thermal and hydrodynamic parameters in a square heat exchanger. Positive enhancement in average heat transfer coefficient (h) and average Nusselt numbers, concerning ZnO@TiO_2/DW composite nanofluids, was exposed for the 0.1 mass% concentration which is about 500–1750 W m^{-2} K.
- The research outcomes explained the presence of both ZnO and TiO_2 nanoparticles in the base fluid cause to enhance the heat transfer properties, which is the best combination for cooling and other applications.

Acknowledgements Authors gratefully acknowledge the UMRG grant RP045C-17AET, UM Research University Grant GPF050A-2018, Institute of Advanced Studies, Nanotechnology and Catalysis Research Center, Department of Mechanical Engineering and the University of Malaya for the support to conduct this research work.

Compliance with ethical standard

Conflict of interest The authors declare that they have no conflict of interests.

References

1. Agarwal DK, Vaidyanathan A, Sunil Kumar S. Investigation on convective heat transfer behaviour of kerosene-Al_2O_3 nanofluid. Appl Therm Eng. 2015;84:64–73.
2. Alyan A, Abdel-Samad S, Massoud A, Waly SA. Characterization and thermal conductivity investigation of Copper-Polyaniline Nano composite synthesized by gamma radiolysis method. Heat Mass Transf. 2019;55(9):1–9.
3. Arote SA, Pathan AS, Hase YV, Bardapurkar PP, Gapale DL, Palve BM. Investigations on synthesis, characterization and humidity sensing properties of ZnO and ZnO–ZrO_2 composite nanoparticles prepared by ultrasonic assisted wet chemical method. Ultrason Sonochem. 2019;55:313–21.
4. Azwadi CSN, Adamu IM, Jamil MM. Preparation methods and thermal performance of hybrid nanofluids. J Adv Rev Sci Res. 2016;24(1):13–23.
5. Bahiraei M, Mazaheri N, Rizehvandi A. Application of a hybrid nanofluid containing graphene nanoplatelet–platinum composite powder in a triple-tube heat exchanger equipped with inserted ribs. Appl Therm Eng. 2019;149:588–601.
6. Blasius H. Grenzschichten in Flüssigkeiten mit kleiner Reibung. Leipzig: Druck von BG Teubner; 1907.
7. Botha SS, Ndungu P, Bladergroen BJ. Physicochemical properties of oil-based nanofluids containing hybrid structures of silver nanoparticles supported on silica. Ind Eng Chem Res. 2011;50(6):3071–7.
8. Choi SUS. Developments and applications of non-Newtonian flows. New York: ASME; 1995. p. 99.
9. Choi SUS, Eastman JA. Enhancing thermal conductivity of fluids with nanoparticles. Lemont: Argonne National Lab; 1995.
10. Dhinesh Kumar D, Valan Arasu A. A comprehensive review of preparation, characterization, properties and stability of hybrid nanofluids. Renew Sustain Energy Rev. 2018;81:1669–89.
11. Esfe MH, Raki HR, Emami MRS, Afrand M. Viscosity and rheological properties of antifreeze based nanofluid containing hybrid nano-powders of MWCNTs and TiO_2 under different temperature conditions. Powder Technol. 2019;342:808–16.
12. Fernandez-Seara J, Uhía FJ, Sieres J, Campo A. A general review of the Wilson plot method and its modifications to determine convection coefficients in heat exchange devices. Appl Therm Eng. 2007;27(17–18):2745–57.
13. Godson L, Raja B, Lal DM, Wongwises S. Enhancement of heat transfer using nanofluids—an overview. Renew Sustain Energy Rev. 2010;14(2):629–41.
14. Hamid KA, Azmi WH, Nabil MF, Mamat R, Sharma KV. Experimental investigation of thermal conductivity and dynamic viscosity on nanoparticle mixture ratios of TiO_2–SiO_2 nanofluids. Int J Heat Mass Transf. 2018;116:1143–52.
15. Hammed NA, Aziz AA, Usman AI, Qaeed MA. The sonochemical synthesis of vertically aligned ZnO nanorods and their UV photodetection properties: effect of ZnO buffer layer. Ultrason Sonochem. 2019;50:172–81.
16. Huminic G, Huminic A. Hybrid nanofluids for heat transfer applications—a state-of-the-art review. Int J Heat Mass Transf. 2018;125:82–103.
17. Jamali M, Toghraie D. Investigation of heat transfer characteristics in the developing and the developed flow of nanofluid inside a tube with different entrances in the transition regime. J Therm Anal Calorim. 2019;139:1–15.
18. Javadzadegan A, Motaharpour SH, Moshfegh A, Akbari OA, Afrouzi HH, Toghraie D. Lattice-Boltzmann method for analysis of combined forced convection and radiation heat transfer in a channel with sinusoidal distribution on walls. Phys A Stat Mech Appl. 2019;526:121066.
19. Kumar N, Sonawane SS. Experimental study of Fe_2O_3/water and Fe_2O_3/ethylene glycol nanofluid heat transfer enhancement in a shell and tube heat exchanger. Int Commun Heat Mass Transf. 2016;78:277–84.
20. Kumar V, Sarkar J. Research and development on composite nanofluids as next-generation heat transfer medium. J Therm Anal Calorim. 2019;137(4):1133–54.
21. Li Z, Barnoon P, Toghraie D, Dehkordi RB, Afrand M. Mixed convection of non-Newtonian nanofluid in an H-shaped cavity with cooler and heater cylinders filled by a porous material: two phase approach. Adv Powder Technol. 2019;30(11):2666–85.
22. Masuda H, Ebata A, Teramae K, Hishinuma N, Ebata Y. Alteration of thermal conductivity and viscosity of liquid by dispersing ultra-fine particles. Dispersion of γ-Al_2O_3, SiO_2 and TiO_2 ultrafine particles. 1993.
23. Mostafazadeh A, Toghraie D, Mashayekhi R, Akbari OA. Effect of radiation on laminar natural convection of nanofluid in a vertical channel with single-and two-phase approaches. J Therm Anal Calorim. 2019;138(1):779–94.
24. Nazari MA, Ghasempour R, Ahmadi MH, Heydarian G, Shafii MB. Experimental investigation of graphene oxide nanofluid on

heat transfer enhancement of pulsating heat pipe. Int Commun Heat Mass Transf. 2018;91:90–4.
25. Nguyen CT, Roy G, Gauthier C, Galanis N. Heat transfer enhancement using Al_2O_3-water nanofluid for an electronic liquid cooling system. Appl Therm Eng. 2007;27(8–9):1501–6.
26. Ouikhalfan M, Labihi A, Belaqziz M, Chehouani H, Benhamou B, Sari A, Belfrika A. Stability and thermal conductivity enhancement of aqueous nanofluid based on surfactant-modified TiO_2. J Dispers Sci Technol. 2019. https://doi.org/10.1080/01932691.2019.1578665.
27. Palacios A, Cong L, Navarro ME, Ding Y, Barreneche C. Thermal conductivity measurement techniques for characterizing thermal energy storage materials—a review. Renew Sustain Energy Rev. 2019;108:32–52.
28. Parrales A, Hernández-Pérez JA, Flores O, Hernandez H, Gómez-Aguilar JF, Escobar-Jiménez R, Huicochea A. Heat Transfer coefficients analysis in a helical double-pipe evaporator: Nusselt number correlations through artificial neural networks. Entropy. 2019;21(7):689.
29. Petukhov BS. Heat transfer and friction in turbulent pipe flow with variable physical properties, Advances in heat transfer. Adv Heat Transf. 1970;6:503–64.
30. Peyghambarzadeh SM, Hashemabadi SH, Hoseini SM, Jamnani MS. Experimental study of heat transfer enhancement using water/ethylene glycol based nanofluids as a new coolant for car radiators. Int Commun Heat Mass Transf. 2011;38(9):1283–90.
31. Phillips SH, Haddad TS, Tomczak, SJ. Developments in nanoscience: polyhedral oligomeric silsesquioxane (POSS)-polymers. Curr Opin Solid State Mater Sci. 2004;8(1):21–9.
32. Ramadhan AI, Azmi WH, Mamat R, Hamid KA, Norsakinah S. Investigation on stability of tri-hybrid nanofluids in water-ethylene glycol mixture. In: IOP Conference Series: Materials Science and Engineering. 2019. 1st International Postgraduate Conference on Mechanical Engineering (IPCME2018), 31 October 2018 , UMP Library, Pekan. pp. 1–9.
33. Ricard D, Roussignol P, Flytzanis C. Surface-mediated enhancement of optical phase conjugation in metal colloids. Opt Lett. 1985;10(10):511–3.
34. Said Z, Sabiha MA, Saidur R, Hepbasli A, Rahim NA, Mekhilef S, Ward TA. Performance enhancement of a flat plate solar collector using titanium dioxide nanofluid and polyethylene glycol dispersant. J Clean Prod. 2015;92:343–53.
35. Saleh R, Putra N, Wibowo RE, Septiadi WN, Prakoso SP. Titanium dioxide nanofluids for heat transfer applications. Exp Therm Fluid Sci. 2014;52:19–29.
36. Saranprabhu MK, Rajan KS. Magnesium oxide nanoparticles dispersed solar salt with improved solid phase thermal conductivity and specific heat for latent heat thermal energy storage. Renew Energy. 2019;141:451–9.
37. Sebastian N, Yu WC, Hu YC, Balram D, Yu YH. Sonochemical synthesis of iron-graphene oxide/honeycomb-like ZnO ternary nanohybrids for sensitive electrochemical detection of antipsychotic drug chlorpromazine. Ultrason Sonochem. 2019;59:104696.
38. Selvakumar RD, Dhinakaran S. Nanofluid flow and heat transfer around a circular cylinder: a study on effects of uncertainties in effective properties. J Mol Liq. 2016;223:572–88.
39. Shah J, Ranjan M, Sooraj KP, Sonvane Y, Gupta SK. Surfactant prevented growth and enhanced thermophysical properties of CuO nanofluid. J Mol Liq. 2019;283:550–7.
40. Shahidi S, Rezaee H, Rashidi A, Ghoranneviss M. In situ synthesis of ZnO Nanoparticles on plasma treated cotton fabric utilizing durable antibacterial activity. J Nat Fibers. 2018;15(5):639–47.
41. Sivasamy P, Harikrishnan S, Jayavel R, Hussain SI, Kalaiselvam S, Lu L. Preparation and thermal characteristics of caprylic acid based composite as phase change material for thermal energy storage. Mater Res Express. 2019;6(10):105051.
42. Sobhan CB, Peterson GP. Microscale and nanoscale heat transfer: fundamentals and engineering applications. Boca Raton: CRC Press; 2008.
43. Sundar LS, Sharma KV, Singh MK, Sousa ACM. Hybrid nanofluids preparation, thermal properties, heat transfer and friction factor—a review. Renew Sustain Energy Rev. 2017;68:185–98.
44. Taha-Tijerina J, Narayanan TN, Gao G, Rohde M, Tsentalovich DA, Pasquali M, Ajayan PM. Electrically insulating thermal nanooils using 2D fillers. ACS Nano. 2012;6(2):1214–20.
45. Taherian H, Alvarado JL, Mohseni Languri E. Enhanced thermophysical properties of multiwalled carbon nanotubes based nanofluids. Part 1: critical review. Renew Sustain Energy Rev. 2018;82:4326–36.
46. Uysal C, Gedik E, Chamkha A. A numerical analysis of laminar forced convection and entropy generation of a diamond-Fe_3O_4/water hybrid nanofluid in a rectangular minichannel. J Appl Fluid Mech. 2019;12(2):391–402.
47. Uysal C, Korkmaz ME. Estimation of entropy generation for Ag–MgO/water hybrid nanofluid flow through rectangular minichannel by using artificial neural network. J Polytech. 2019;22(1):41–51.
48. Varzaneh AA, Toghraie D, Karimipour A. Comprehensive simulation of nanofluid flow and heat transfer in straight ribbed microtube using single-phase and two-phase models for choosing the best conditions. J Therm Anal Calorim. 2020;139:1–20.
49. Waini I, Ishak, A., Pop, I. Unsteady flow and heat transfer past a stretching/shrinking sheet in a hybrid nanofluid. Int J Heat Mass Trans. 2019;136:288–97.
50. Wang Y, Zhang X, Ji J, Li Y, Munyalo JM, Liu B. Thermal conductivity modification of n-octanoic acid-myristic acid composite phase change material. J Mol Liq. 2019;288:111092.
51. Zawawi NNM, Azmi WH, Redhwan AAM, Sharif MZ, Samykano M. Experimental investigation on thermo-physical properties of metal oxide composite nanolubricants. Int J Refrig. 2018;89:11–21.